

# Off-Resonance Effects in Two-Dimensional NQR Spectroscopy Using a Single Crystal

T. G. Ajithkumar,\* K. V. Ramanathan,† P. C. Mathias,† and Anil Kumar\*\*†<sup>1</sup>

\*Department of Physics and †Sophisticated Instruments Facility, Indian Institute of Science, Bangalore 560 012, India

Received February 4, 1998; revised June 9, 1998

**Two-dimensional nutation pure NQR experiments on <sup>35</sup>Cl have been carried out on a single crystal of NaClO<sub>3</sub>. The 2D nutation experiment separates out different orientations of each chemically equivalent site in a unit cell as a separate frequency in the  $\omega_1$  domain. The squares of the observed frequencies lie on a straight line with respect to the squares of the offsets, confirming the expected offset dependence quantitatively. The intercepts at zero offset yield the relative orientations of the efg tensors with respect to the axis of the radiofrequency coil.** © 1998 Academic Press

## INTRODUCTION

Recently two-dimensional nutation nuclear quadrupolar resonance (NQR) experiments have been described in which the two-dimensional time-domain signal  $S(t_1, t_2)$  is detected during the free induction decay (FID) for time  $t_2$  for varying radiofrequency (rf) pulse widths  $t_1$  (1, 2). These experiments have the advantage that the nutation frequencies of chemically equivalent but physically inequivalent (identical electric field gradient (efg) tensors being oriented in different directions) sites are different, leading to a resolution and identification of such sites. The off-resonance effects in such experiments have also recently been described (3–5). Most of these experiments were carried out on powder samples leading to broad two-dimensional contours. These broad contours were compared with simulated contours, qualitatively confirming the offset dependence (3–5). This paper describes experiments carried out on a single crystal, leading to quantitative comparison with theory. These experiments confirm the offset dependence and opens the way to obtaining detailed information on various chemically equivalent but physically inequivalent sites in a crystal.

The experiments have been carried out using a single crystal of NaClO<sub>3</sub>. The pure NQR of <sup>35</sup>Cl is observed at 29.92 MHz and is an extremely well-studied resonance (6–9).

The Hamiltonian in the nutation period is given by

$$H = H_Q + H_{\text{rf}}. \quad [1]$$

$H_Q$  is the Hamiltonian in the absence of rf given by (10)

$$H_Q = \frac{e^2qQ}{4I(2I-1)} \left[ 3I_z^2 - I(I+1) + \frac{\eta}{2}(I_+^2 + I_-^2) \right], \quad [2]$$

where  $eq = \partial^2V/\partial z^2$  is the electric field gradient,  $Q$  is the quadrupole moment,  $I$  is the nuclear spin,  $\eta$  is the asymmetry parameter, and  $H_{\text{rf}}$  is given by

$$H_{\text{rf}} = -\gamma H_1 \cos \omega t \times [I_x \sin \theta \cos \phi + I_y \sin \theta \sin \phi + I_z \cos \theta], \quad [3]$$

where  $\gamma H_1$  is the amplitude of the rf,  $\omega$  is its frequency, and  $\theta, \phi$  are the angles the rf field makes with the principal axis of the efg tensor.

## THEORY

The pulse sequence used for the two-dimensional nutation pure NQR spectroscopy is given in Fig. 1a. Here the rf field is present during the evolution period  $t_1$ . The detection period  $t_2$  consists of pure NQR evolution in the absence of rf fields. The two-dimensional signal in the experiment, after phase-sensitive detection, is obtained as (4, 5, 10)

$$S(t_1, t_2) = \frac{\omega_R}{4\zeta} \mathcal{R}^2(\theta, \phi) [\sin 2\zeta t_1 \sin(\Delta\omega t_2 + \psi) - \frac{\Delta\omega}{2\zeta} (1 - \cos 2\zeta t_1) \cos(\Delta\omega t_2 + \psi)], \quad [4]$$

<sup>1</sup> To whom correspondence should be addressed. E-mail: anilnmr@physics.iisc.emet.in.

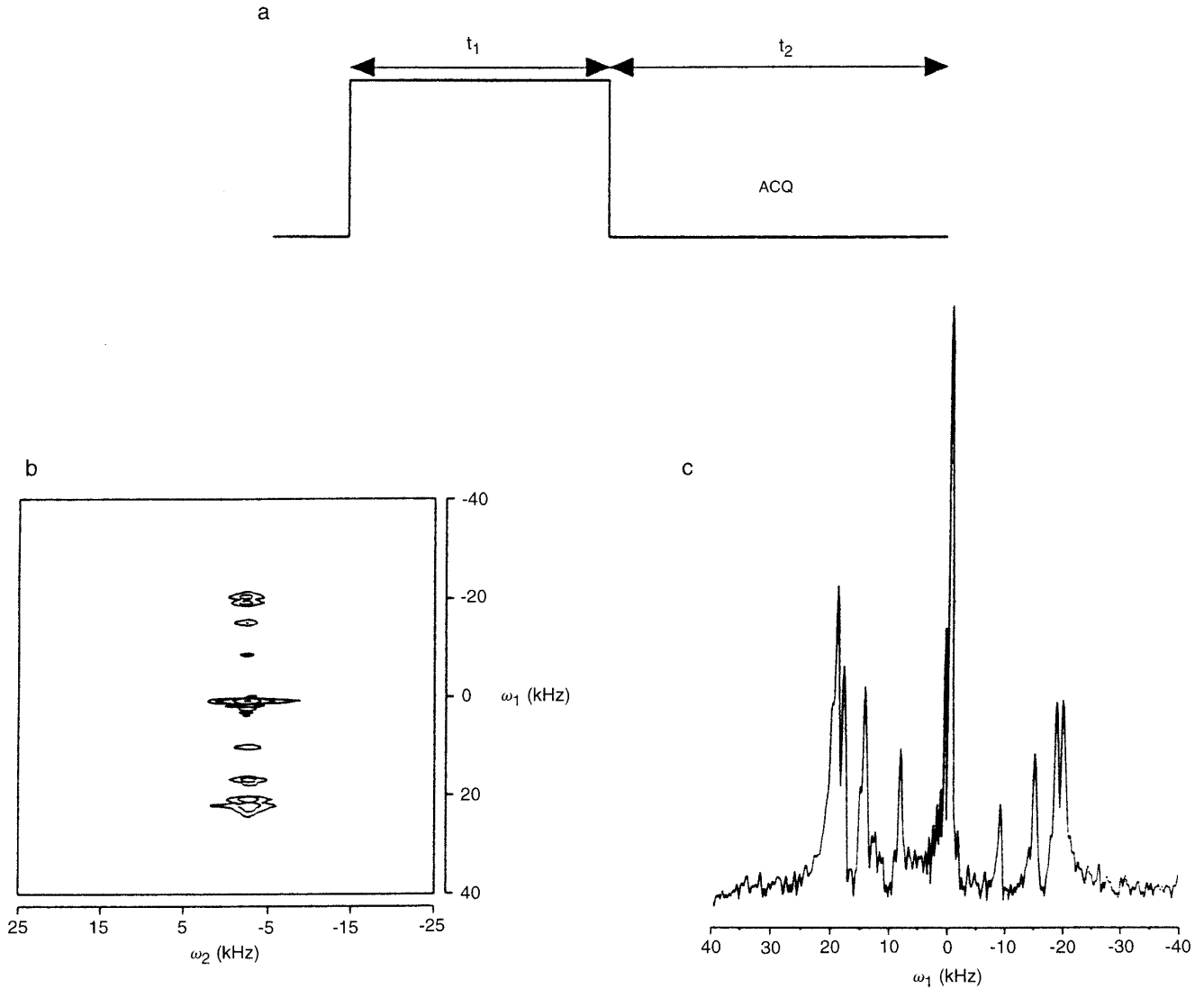


**FIG. 1.** (a) The pulse sequence for the 2D nutation NQR spectroscopy. (b) Absolute intensity contour plot of the 2D nutation NQR spectrum, obtained with the pulse sequence of (a). The rf offset in this experiment was 2.0 kHz. (c) A cross section from the 2D nutation NQR spectrum of (b) taken parallel to  $\omega_1$  at  $\omega_2 = -2$  kHz.

where

$$\Delta\omega = \omega - \omega_0$$

$$\omega_R = \gamma H_1$$

$$2\xi = \sqrt{4m^2 + \Delta\omega^2}$$

$$m = \frac{\omega_R \mathcal{R}(\theta, \phi)}{4\sqrt{3 + \eta^2}}$$

$$\mathcal{R}(\theta, \phi) = [4\eta^2 \cos^2\theta + \sin^2\theta \\ \times (9 + \eta^2 + 6\eta \cos 2\phi)]^{1/2}$$

and  $\omega_0$  for spin  $I = \frac{3}{2}$  is

$$\omega_0 = \frac{e^2 q Q}{2\hbar} \left(1 + \frac{\eta^2}{3}\right)^{1/2}. \quad [10]$$

[6]

[7]

[8]

[9]

It may be pointed out that Eq. [4] differs from earlier results (3, 4), which used the original calculation of the NQR signal by Pratt *et al.* (10). Recently Mackowaik and Katowski (5) pointed out that Pratt *et al.* calculated the expectation values of operators  $\langle I_Q \rangle$  in the laboratory frame, but with the expansion coefficients in the rotating frame, resulting in an error of the factor of  $\exp(i(\omega_i - \omega_j)t_w)$  in the signal, where  $t_w$  is the pulse width and  $(\omega_i - \omega_j)$  is the resonance frequency. This causes

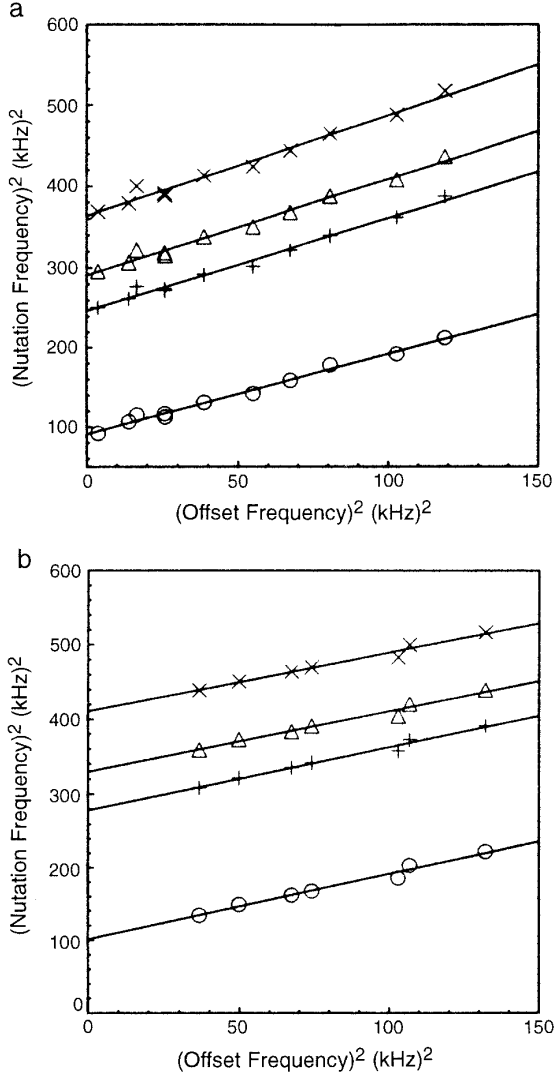


**FIG. 2.** (a) Plot of the square of the  $\omega_1$  frequency versus  $\Delta\omega^2$  for positive  $\Delta\omega$ . The 2D experiments were carried out for 11 different offsets. The four straight lines correspond to four different sites in the unit cell. The data fit the straight lines having slopes of 1.04, 1.14, 1.18, and 1.24, respectively, for intercepts of 90.8, 246.8, 290.8, and 363.5 (kHz) $^2$ . (b) Plot of the square of the  $\omega_1$  frequency versus  $\Delta\omega^2$  for negative  $\Delta\omega$ . The 2D experiments were carried out for 7 different offsets. The four straight lines again correspond to four different sites in the unit cell. The data fit the straight lines having slopes of 0.90, 0.80, 0.81, and 0.79, respectively, for intercepts of 101.2, 278.3, 329.6, and 410.8 (kHz) $^2$ .

little error in one-dimensional experiments where  $t_w$  is small, but becomes crucial in two-dimensional experiments, where it is a variable parameter. We have recalculated the time evolution of the magnetization according to Fig. 1a ab initio and the result is given in Eq. [4]. Equation [4] is also more general than that given by Mackowiak and Katowski (5).

Equation [4] states that in the  $\omega_1$  dimension, there is a zero-frequency component of amplitude  $(\Delta\omega/2\zeta)$ , an absorptive component at  $\pm 2\zeta$  of amplitude  $(\Delta\omega/2\zeta)$ , and a dispersive

component at  $\pm 2\zeta$  whose amplitude is not dependent on  $\Delta\omega$ . All these components have mixed phase (for arbitrary  $\psi$ ) in the  $\omega_2$  domain and occur at  $\omega_2 = -\Delta\omega$ .

From Eq. [7], the square of the nutation frequency in the  $\omega_1$  domain can be written as

$$(2\zeta)^2 = 4m^2 + (\Delta\omega)^2 \quad [11]$$

and a plot of  $(2\zeta)^2$  versus  $(\Delta\omega)^2$  yields a straight line of slope unity and intercept given by  $4m^2$ . This intercept depends on  $\theta$ ,  $\phi$ , and  $\eta$ . However, for  $\eta = 0$ , it depends only on  $\theta$  and is given by

$$4m^2 = \frac{3}{4} \omega_R^2 \sin^2 \theta. \quad [12]$$

In single crystals, such intercepts yield relative orientations of chemically equivalent tensors.

## EXPERIMENT

Two-dimensional nutation NQR experiments were carried out using an MSL-300 solid-state NMR spectrometer without the magnet. A solenoid rf coil, in the place of the stator of a magic angle spinning Bruker probe, was used. For good rf homogeneity, a small crystal of  $\text{NaClO}_3$  (dimension  $4 \times 2 \times 2$  mm) was placed at the center of a long coil (length 30 mm, inner diameter 8 mm having 12 turns) using Teflon spacers. The absolute intensity 2D spectrum for an arbitrary rf field with offset  $(\Delta\omega) = 2.0$  kHz is shown in Fig. 1b. There is a single frequency in the  $\omega_2$  domain and four frequencies in each quadrant of  $\omega_1$  along with a zero-frequency component. The amplitude of the zero-frequency component increases with the increasing offsets in confirmation with Eq. [4]. The experiment was repeated for various values of rf offsets, in both the negative and the positive directions, for a constant rf amplitude. A cross section of the 2D spectrum (Fig. 1b) parallel to  $\omega_1$  taken at  $\omega_2 = -\Delta\omega$  is shown in Fig. 1c. The exact frequencies of various lines have been obtained from such cross sections. The square of the  $\omega_1$  frequencies  $(2\zeta)^2$  is plotted

**TABLE 1**  
**The Ratio of Square Roots of the Intercepts ( $=m_i/m_1$ ) of the  $(\omega_1)^2$  vs  $(\Delta\omega)^2$  Plots (Figs. 2a and 2b) and the Best Fit  $\sin \theta_i/\sin \theta_1$  Values Obtained Using the Crystal Structure Data**

$i$	rf offset		$\sin \theta_i/\sin \theta_1$
	Negative $m_i/m_1$	Positive $m_i/m_1$	
2	1.66	1.64	1.65
3	1.81	1.79	1.79
4	2.02	2.00	2.00

versus  $(\Delta\omega)^2$  in Fig. 2a for positive  $\Delta\omega$  and in Fig. 2b for negative  $\Delta\omega$ . These plots yield straight lines, confirming the offset dependence of the nutation frequency as given by Eq. [4].<sup>2</sup> The ordinate of these lines gives the nutation frequency for  $\Delta\omega = 0$ , which is related to the strength of the rf field and the orientation of the efg tensor with respect to the coil axis.

The ratios of various intercepts yields  $\mathcal{R}^2(\theta_i, \phi_i)/\mathcal{R}^2(\theta_j, \phi_j)$ , which for  $\eta = 0$  are  $\sin^2\theta_i/\sin^2\theta_j$ . Assuming  $\eta = 0$ , the square roots of these ratios are given in Table 1 for positive and negative offsets.

The orientation of the four physically inequivalent efg tensors with reference to the axis of the rf coil can be obtained as follows. The  $z$  component of the efg tensor has been assumed to be along the Na–Cl bond. From the crystal structure (11), the orientation of these bonds is known. By allowing the orientation of the rf coil axis to span the entire range of direction cosines, the ratios  $\sin\theta_2/\sin\theta_1$ ,  $\sin\theta_3/\sin\theta_1$ , and  $\sin\theta_4/\sin\theta_1$  have been calculated and compared with the experimental values given in Table 1. From these calculations, the orientations of the principal axes of the four efg tensors, with respect to the rf coil axis, turn out to be at  $\theta = (150.7; 54.3; 61.5; 110.7)$  or equivalently at  $\theta = (29.3; 125.7; 118.5; 69.3)$ . The amplitude of the applied rf,  $\omega_R$ , calculated for positive  $\Delta\omega$  experiment, Fig. 2a, is  $22.7 \pm 1$  kHz and for negative  $\Delta\omega$  experiment, Fig. 2b, is  $24.0 \pm 1$  kHz.

<sup>2</sup> The slopes of these lines are not exactly unity but slightly different: more than unity for positive  $\Delta\omega$  and less than unity for negative  $\Delta\omega$ .

## CONCLUSIONS

The offset dependence of NQR nutation frequencies has been studied using a single crystal of  $\text{NaClO}_3$  and the orientations of the four chemically equivalent quadrupolar tensors per unit cell have been obtained, for the first time, from such studies.

## ACKNOWLEDGMENT

Ms. Suja Elizabeth's help in growing and cutting the single crystal is gratefully acknowledged.

## REFERENCES

1. G. S. Harbison, A. Slokenbergs, and T. M. Barbara, *J. Chem. Phys.* **90**(10), 5292 (1989).
2. G. S. Harbison and A. Slokenbergs, *Z. Naturforsch. A* **45**, 575 (1990).
3. J. Dolisnek, F. Milla, G. Papavassiliou, G. Papantopoulos, and R. Rumm, *J. Magn. Reson. A* **114**, 147 (1995).
4. N. J. Sinjavsky, *Z. Naturforsch. A* **50**, 957 (1994).
5. M. Mackowiak and P. Katowski, *Z. Naturforsch. A* **51**, 337 (1996).
6. R. Livingston, *Science* **118**, 61 (1953).
7. Y. Ting, E. R. Manring, and D. Williams, *Phys. Rev.* **96**, 408 (1954).
8. T. C. Wang, *Phys. Rev.* **99**, 566 (1955).
9. H. Zeldes and R. Livingston, *J. Chem. Phys.* **26**, 351 (1957).
10. J. C. Pratt, P. Raghunathan, and C. A. McDowell, *J. Magn. Reson.* **20**, 313 (1975).
11. C. Aravindakshan, *Z. Kristallogr. Bd.* **111**, 241 (1959).